Journal of the Optical Society of Korea
Vol. 13, No. 4, December 2009, pp. 423-427

DOI: 10.3807/JOSK.2009.13.4.423

THz Filter Using the Transverse-electric (TE_1) Mode of the Parallel-plate Waveguide

Eui Su Lee and Tae-In Jeon*

Division of Electrical and Electronics Engineering, Korea Maritime University, 1 Dongsam-dong, Youngdo-gu, Busan 606-791, Korea

(Received October 23, 2009 : revised November 17, 2009 : accepted November 17, 2009)

The results of the experimental and theoretical studies conducted on terahertz filtering using two parallel-plate waveguides (PPWGs) are presented herein. The first PPWG with 355 μm plate separation generates 4 THz bandwidth TM modes (TM_0, TM_2, and TM_4), whereas the second PPWG with 100 μm plate separation operated the THz filter for the generated TM modes with 1.5 THz cutoff frequency. The outgoing THz wave of the two PPWGs was truncated until 1.5 THz, and the system was operated using a high-pass THz filter. The absorption and dispersion of the combined TM and TE modes for the filtering system were calculated. The theoretical calculation and measurement results for the cutoff and oscillation frequency in the spectrum domain agreed well.

Keywords : THz filter, Terahertz, Waveguide, Mode, Parallel-plate
OCIS codes : (040.2235) Far infrared or terahertz; (120.2440) Filters; (070.2615) Frequency filtering; (030.4070) Modes; (230.7390) Waveguides, planar

I. INTRODUCTION

The broadband coupling of freely propagating terahertz (THz) pulses into circular [1] and rectangular [1, 2] metal waveguides, single-crystal sapphire fiber [3], plastic ribbon [4], parallel-plate waveguides (PPWGs) [5], and coaxial cables [6] was recently demonstrated. As the THz pulses propagated through dielectric materials like single-crystal sapphire fiber, plastic ribbon, and coaxial-cable waveguides, the absorption by the dielectric material turned out to be much bigger than that of the waveguide itself. The air-filled PPWG has many advantages when used for the propagation of THz pulses, such as the fact that it has a small power absorption coefficient and a good guiding property when the plate gap is optimized. The concentrated THz energy in the air gap of PPWG can make many THz applications possible, such as spectroscopy [7, 8], photonic waveguide [9], and surface plasmon coupling [10, 11]. As a two-wire coplanar line and a coaxial line, the THz wave of PPWG propagates through the air gap between two metal surfaces.

When the THz wave is coupled at metal surfaces that are not optically smooth, the electric-field distribution to the air will decay exponentially. This is known as an "evanescent field". If the two metal surfaces are farther separated from each other compared to the 1/e extent of the evanescent field, the evanescent field of one metal surface will not affect that of the other. If the metal surfaces of the PPWGs are sufficiently close to each other, however, their evanescent fields will affect each other. Therefore, the field will create transverse-electric (TE) or transverse-magnetic (TM) modes depending on the polarization of the incoming field. The cutoff frequencies caused by the gap size of the PPWG exist in the TE and TM modes. The extreme group velocity dispersion near the cutoff frequency induces the excessive broadening of sub psec THz pulses. The pulses would not broaden for the transverse-electromagnetic (TEM) modes (known as "TM_0 mode") of the two-wire coplanar line, coaxial line, and PPWG because the TEM mode does not have a cutoff frequency [12]. If the cutoff frequencies of the TM_1 and TM_2 modes are bigger than the bandwidth of a system, only the TEM mode exists [5]. If the cutoff frequencies are smaller than the bandwidth of the system, the TEM and higher TM modes exist at the same time, and the high TM modes cannot be separated from the TEM mode. The lowest-order TE_1 mode of the PPWG can be used as a high-pass filter, however, because the THz wave is totally absorbed below the cutoff frequency.

*Corresponding author: jeon@hhu.ac.kr

Recently, a THz spreading filter has been reported using one-dimensional dielectric multilayer structures [13], however, a THz filter for a freely propagating THz beam has not been reported. In this study, TEM and higher TM modes were generated via perpendicular polarization between the incident THz beam and PPWG. The generated low-frequency component of the modes was filtered by the TE_1 mode, which acted as a high-pass filter.

II. EXPERIMENT

Two sets of PPWGs were inserted between two paraboloidal mirrors to generate TM and TE modes, as shown in Fig. 1, where the THz wave is horizontal-polarized. Since the cylindrical silicon lens used is 15 mm long, 7.07 mm height, and had a 5 mm radius, only the 15×10-mm cross-section of the THz field was open to the PPWGs. Since much of the THz field energy and most of the high-frequency components were concentrated at the center of the THz beam, the opened cross-section was enough for measurement purposes. The first and third silicon lenses placed the line focus of the incoming THz beam on the gap of the PPWG, and the second and fourth silicon lenses produced parallel propagation to the outgoing THz beam where the size of each PPWG was 29.7×40×10 mm.

The cutoff frequencies of the TM and TE modes are given by $f_c=mc/2d$, where m is the number of high-order modes, c the speed of light, and d the plate separation of the PPWGs. The first PPWG (with 355 μm plate separation) was set perpendicular to the polarization of the incoming THz wave to generate the TM mode. Therefore, the propagated THz pulse had a TM_0 (TEM) mode with low loss and negligible group velocity dispersion. The THz pulse also had higher even modes, such as TM_2 and TM_4, with 0.845 and 1.69 THz cutoff frequencies, respectively. As the input pulse had Gaussian field distribution, TM_1 and TM_3, which had odd field patterns, could not be easily coupled. Moreover, the dipole receiver antenna can detect only even field patterns; it cannot detect the odd modes in the system [14].

Fig. 2(a) and (b) show the measured THz pulse and spectrum. The first THz pulse shown indicates the TEM mode, and the delayed oscillations indicate higher TM_2 and TM_4 modes because of their slow group velocities. The inset figure shows an extension of the oscillation from 120 psec to 160 psec. The amplitude of each oscillation was continuously reduced with increasing time because the low-frequency components had slow group velocity and a high absorption coefficient. The slow-group-velocity components continually oscillated after 160 psec, but they could not be measured because of the THz pulse reflected from the cylindrical silicon lens. Most of the THz TM modes, however, were within 160 psec. The spectrum clearly shows the modes' components. The envelope of the amplitude spectrum indicates the TEM mode. The TM_2 and TM_4 modes were observed with the oscillation starting at the cutoff frequencies of 0.845 and 1.690 THz, respectively. The TM_6 mode with 2.535 THz cutoff frequency was not clearly shown because of the limited THz beam power. The inset figure shows the spectrum oscillations near the TM_4 mode. The tail part of the TM_2 mode had large periodic repetition while the head part of the TM_4 mode had short periodic repetition starting at the 1.690 THz cutoff frequency. In this study, an attempt was made to remove the signal

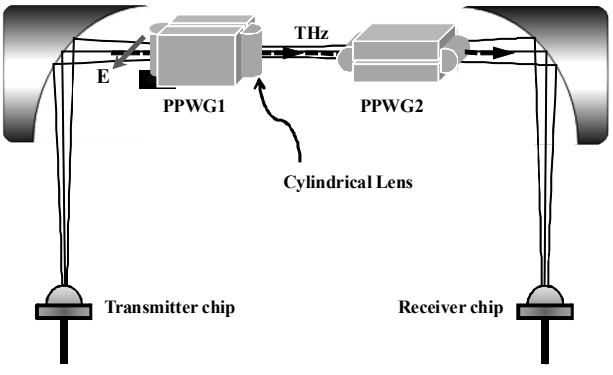

FIG. 1. Schematic diagram of the THz parallel-plate waveguide system.

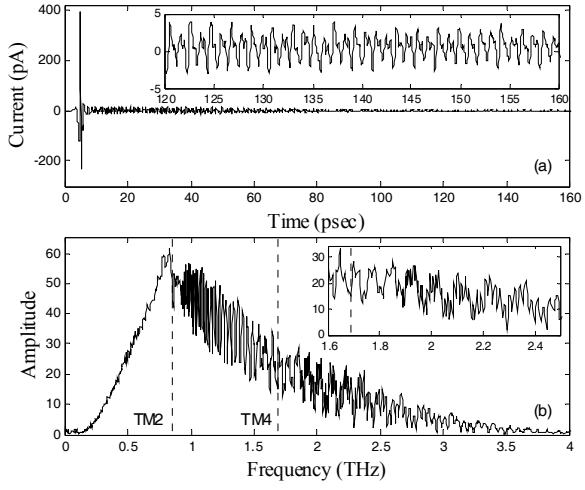

FIG. 2. Measurements for the TM mode with 355 μm plate separation. (a) TM mode THz pulse in the time domain. The inset shows an extension of the oscillation from 120 psec to 160 psec. (b) Amplitude spectrum of the TM mode THz pulse. The envelope of the amplitude spectrum indicates the TM_0 mode. The inset shows the spectrum from 1.6 THz to 2.5 THz. The cutoff frequencies for the TM modes are indicated by the dotted vertical lines.

below 1.5 THz (cutoff frequency), using a TE_1–mode-type high-pass filter.

The second PPWG with 100 μm plate separation was set parallel to the polarization of the incoming THz wave to generate a TE mode that determines the 1.5 THz cutoff frequency for the TE_1 mode. Since the TE_2 mode (3 THz cutoff frequency) had an odd field pattern, the system cannot be easily coupled and detected. The group velocity dispersion of the TE mode was very high after the cutoff frequency and slowly approached the speed of light with increasing frequency [12]. The high-frequency components of the pulse arrived first, and the low-frequency components after the cutoff frequencies were delayed. Therefore, the time domain pulse was stretched and expanded to more than 100 psec, with a negative chirp, as shown in Fig. 3(a). As there was no TEM component, only the oscillation of the TE_1 mode component was detected in the time domain. The oscillation after 100 psec was ignored because its magnitude was too small compared to the maximum magnitude of the oscillation around 10 psec. The inset figure shows the extension of the oscillation by the group velocity dispersion for the head parts of the oscillation. Fig. 3(b) shows the spectrum of the time domain THz pulse. The low frequency was truncated at the cutoff frequency, and the spectrum extended up to 4 THz. The spectrum response was a high-pass filter with frequency-dependent gain. The stop-band and pass-band edges were 1.5 and 1.72 THz, respectively, as shown by the dashed vertical lines. Therefore, the transition bandwidth (rising frequency) was about 0.22 THz. The transition bandwidth usually depends on the alignment of the PPWG. Bad alignment

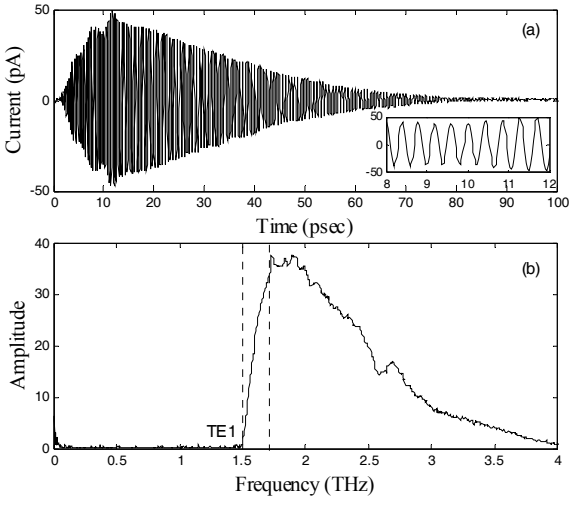

FIG. 3. Measurements for the TE mode with 100 μm plate separation. (a) TE_1 mode THz pulse in the time domain. The inset shows the extension of the oscillation from 8 psec to 12 psec. (b) Amplitude spectrum of the TE_1 mode THz pulse.

of the PPWG has a large transition bandwidth. When PPWG1 and PPWG2 are in a series setting, as shown in Fig. 1, the spectrum of the TM mode is filtered by the TE_1 mode.

The analytic expressions of phase velocity V_Φ and group velocity V_g are given by [12]

$$V_\Phi = V \Big/ [1-(\lambda/\lambda_c)^2]^{1/2}, \quad (1)$$

$$V_g = V \cdot [1-(\lambda/\lambda_c)^2]^{1/2}, \quad (2)$$

where $V=1/\sqrt{\mu\varepsilon}$ and λ_c is the wavelengths at the cutoff frequency. The speed of light can be expressed as $V=\sqrt{V_\Phi \cdot V_g}$. The magnitude of V_Φ in a given mode is infinite at the cutoff frequency because the denominator is zero, as shown in eq. (1). Moreover, the magnitude of V_g in a given mode is zero at the cutoff frequency, as shown in eq. (2). The velocities of V_Φ and V_g before the cutoff frequencies are infinite and zero, respectively, and the velocities approach the speed of light after the cutoff frequencies, with increasing frequency. The combined phase or group velocities for the TM and TE modes can be obtained using the equation

$$V_{\Phi,g\_TMTE} = 2\cdot(V_{\Phi,g\_TM}\cdot V_{\Phi,g\_TE}) \Big/ (V_{\Phi,g\_TM}+V_{\Phi,g\_TE}), \quad (3)$$

where V_{Φ,g_TM} and V_{Φ,g_TE} are the phase or group velocity for the TM and TE modes, respectively. Fig. 4(a) shows the phase and group velocity of the combined TM and TE modes. Fig. 4(b), on the other hand, shows the absorption coefficient of the combined TM and TE modes. The vertical dashed lines indicate the cutoff frequency of the TE_1 mode. The even modes detected by the first PPWG were TM_0, TM_2, and TM_4, and the odd mode detected by the second PPWG was TE_1 until 4 THz bandwidth, whereas V_Φ and V_g of the TM_0 mode were constant at the speed of light. Therefore, the TM_0+TE_1 mode is the same as the TE_1 mode, as shown by the thick solid lines, and the other combined components were the even TM modes+TE_1 (TM_2+TE_1, TM_4+TE_1, TM_6+TE_1, etc.), as shown by the thin solid lines in Fig. 4(a). The dashed lines indicate the odd TM modes+TE_1 combinations. The combined mode lines diverged farther away from each other with increasing frequency because V_Φ and V_g of TE_1 mode approached the speed of light.

Since the absorption coefficient of the TE_1 mode was infinite before the cutoff frequency, the combined spectrum with the TM modes was truncated up until

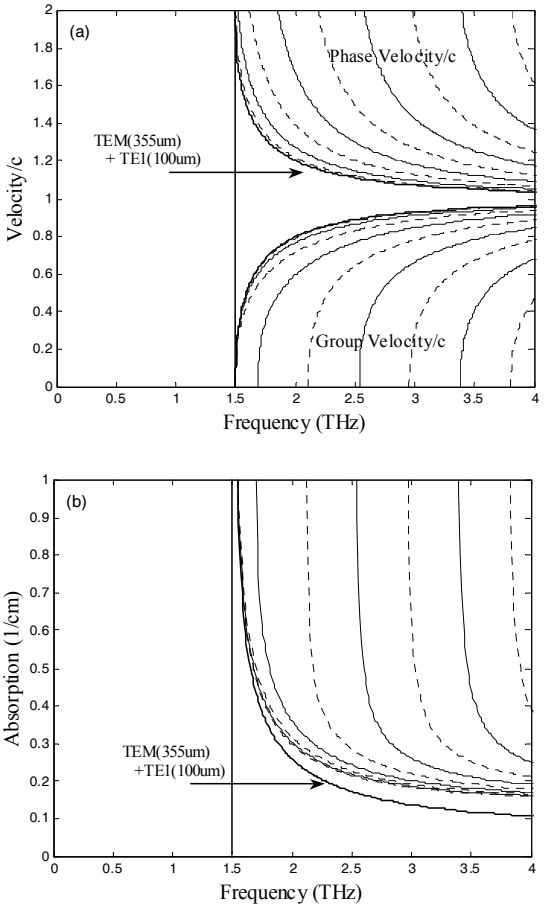

FIG. 4. Combined TM and TE modes. The dashed curves indicate the combined odd TM modes and TE_1 mode, and the solid curves indicate the combined even TM modes and TE_1 mode. (a) Phase and group velocities for the TM_m+TE_1 modes. (b) Field absorption for the TM_m+TE_1 modes. The cutoff frequency for the TE_1 mode with 100 μm plate separation is shown by the dashed vertical lines.

the cutoff frequency. The thick solid line in Fig. 4(b) indicates the combined TM_0+TE_1 mode. The dashed and solid thin lines indicate the odd and even TM modes combined with the TE_1 mode, respectively. As the absorption coefficient of the TM_0 mode slightly increased with increasing frequency, the margin between the thick solid line and the first thin dashed line also increased with increasing frequency. Since the absorption coefficient of the TE_1 mode after the cutoff frequency slowly decreased, unlike the TM modes, the combined lower modes approached each other.

The THz wave propagated through PPWG1 and PPWG2 is shown in Fig. 5(a). The inset shows the extended THz wave from 39 psec to 53 psec. The main THz pulse disappeared, and the amplitude of each oscillation was irregular because of the combination of TM and TE modes. The main THz pulse, which corresponds to the TM_0 mode, went out first from

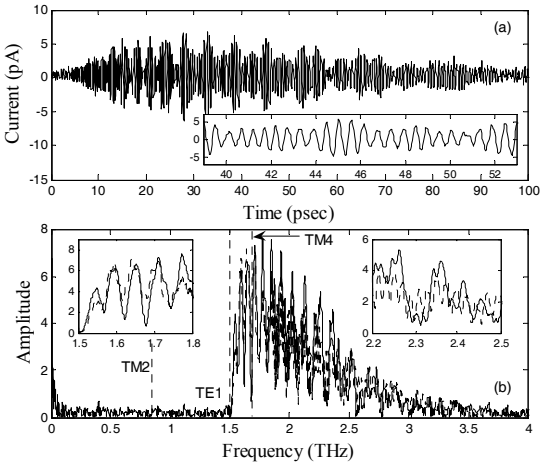

FIG. 5. Measurements (solid lines) and theoretical predications (dots) for the parallel-plate waveguide at TM_m+TE_1. (a) TM_m+TE_1 mode THz pulse in the time domain. The inset shows an extension of the oscillation from 39 psec to 53 psec. (b) Amplitude spectrum of the TM_m+TE_1 mode THz pulse. The envelope of the amplitude spectrum indicates the TE_1 mode. The inset shows an extension of the spectrum from 1.5 THz to 1.8 THz and from 2.2 THz to 2.5 THz.

PPWG1 because its group velocity is equal to the speed of light. When the TM_0 mode came into PPWG2, it was converted to the TE_1 mode. Therefore, the outgoing THz wave from PPWG2 did not have the main THz pulse. Fig. 5(b) shows the spectrum that clearly shows the filtering of the low-frequency component. The spectrum was truncated before the cutoff frequency of the TE_1 mode. Part of TM_2 and TE_1 was detected because the cutoff frequency of TE_1 was at the TM_2 mode bandwidth. Moreover, (TM_2+TM_4)+TE_1 can be detected by the system.

The spectrum of the outgoing THz wave from PPWG is given by [14]

$$E_{outTM_mTE_1}(\omega) = E_{ref}(\omega)\sum_{m=0}^{TM_m} Ke^{-j(\beta_{g,m}-2\beta_0)L}e^{-\alpha_m L}, \qquad (4)$$

where T_m and C_m are the total transmission and coupling coefficient of the entrance and exit waveguides, respectively. The constant $K = T_{TM_m}{C_{TM_m}}^2 T_{TE_1}{C_{TE_1}}^2$ parameter was used for fitting. $\alpha_m = \alpha_{TM_m} + \alpha_{TE_1}$ is the amplitude absorption coefficient shown in Fig. 4(b). $\beta_{g,m} = \beta_{g,TM_m} + \beta_{g,TE_1}$ is the propagation constant related to the phase and group velocities shown in Fig. 4(a), and β_0 is the phase constant. Using theoretical calculation, the obtained spectrum is shown by the dashed line in the inset figures. The measured oscillated components of the combined modes (after the cutoff frequency) agree well with the calculation result. The amplitudes

of the oscillations are not in agreement, though, especially for the high-frequency component, due to the coupling constant. The filtering effect on the spectrum domain was well observed, however, not only in the experiment but also in the theoretical results.

III. CONCLUSION

In this study, the THz filtering effect on the TE mode was investigated for the first time. The generated TM modes with 355 μm PPWG plate separation were well-defined TM_0, TM_2, and TM_4 modes. As the bandwidth of the TM_0 mode extended up to 4 THz frequency, TM modes are considered good for incoming THz reference waves, to filter their low-frequency components. Moreover 100 μm PPWG plate separation produces a TE_1 mode with 1.5 THz cutoff frequency when the incoming THz polarization and the surface of the PPWG are parallel to each other. The spectrum of the TE_1 mode is truncated before the cutoff frequency because of the infinite absorption coefficient and the absence of a TEM component. When the first and second PPWGs are series-set between two paraboloidal mirrors in the THz system, the TM modes with a 4 THz bandwidth are truncated until 1.5 THz, which is the cutoff frequency of the TE_1 mode from the second PPWG. The system is operated as a high-pass filter. The THz filtering effect was also demonstrated using theoretical calculation, which applies the combined TM and TE modes for the absorption and dispersion of the filtering system. Even though the amplitude of the measurement and calculation was slightly deviant, the cutoff frequency and oscillations agreed well. The THz filtering system is expected to be used in THz logic and sensing systems in the future.

ACKNOWLEDGMENT

This work was accomplished with support from the Korea Research Foundation Grant funded by the Korean government (MOEHRD, Basic Research Promotion Fund) (KRF-2008-521-C00115), and from MKE (The Ministry of Knowledge Economy), Korea, under the ITRC (Information Technology Research Center) support program supervised by the NIPA (National IT Industry Promotion Agency) (NIPA-2009-C1090-0903-0007).

REFERENCES

1. R. W. McGowan, G. Gallot, and D. Grischkowsky, "Propagation of ultra-wideband, short pulses of THz radiation through sub-mm diameter circular waveguides," Opt. Lett. **24**, 1431-1433 (1999).
2. G. Gallot, S. P. Jamison, R. W. McGowan, and D. Grischkowsky, "THz waveguides," J. Opt. Soc. Am. B **17**, 851-863 (2000).
3. S. P. Jamison, R. W. McGowan, and D. Grischkowsky, "Single-mode waveguide propagation and reshaping of sub-ps terahertz pulses in sapphire fibers," Appl. Phys. Lett. **76**, 1987-1989 (2000).
4. R. Mendis and D. Grischkowsky, "Plastic ribbon THz waveguides," J. Appl. Phys. **88**, 4449-4451 (2000).
5. R. Mendis and D. Grischkowsky, "Undistorted guided wave propagation of sub-picosecond THz pulses," Opt. Lett. **26**, 846-848 (2001).
6. T.-I. Jeon and D. Grischkowsky, "Direct optoelectronic generation and detection of subps electrical pulses on sub-mm coaxial transmission lines," Appl. Phys. Lett. **85**, 6092-6094 (2004).
7. M. Nagel, P. H. Bolivar, and H. Kurz, "Modular parallel-plate THz components for cost efficient biosensing systems," Semicond. Sci. Technol. **20**, 281-285 (2005).
8. N. Laman, S. S. Harsha, D. Grischkowsky, and J. S. Melinger, "7 GHz resolution waveguide THz spectroscopy of explosives related solids showing new features," Opt. Exp. **16**, 4094-4105 (2008).
9. Z. P. Jian, J. Pearce, and D. M. Mittleman, "Two-dimensional photonic crystal slabs in parallel-plate metal waveguides studied with terahertz time-domain spectroscopy," Semicond. Sci. Technol. **20**, S300-S306 (2005).
10. T.-I. Jeon and D. Grischkowsky, "THz Zenneck surface wave (THz surface plasmon) propagation on a metal sheet," Appl. Phys. Lett. **88**, 061113 (2006).
11. M. Gong, D. Grischkowsky, and T.-I. Jeon, "THz surface wave collapse on coated metal surfaces," Opt. Exp. **17**, 17088-17101 (2009).
12. N. Marcuvitz, *Waveguide Handbook* (Peregrinus, London, UK, 1986).
13. M. Yi, Y. Kim, D.-S. Yee, and J. Ahn, "Terahertz frequency spreading filter via one-dimensional dielectric multilayer structures," J. Opt. Soc. Korea **13**, 398-402 (2009).
14. E. S. Lee, J. S. Jang, S. H. Kim, Y. B. Ji, and T.-I. Jeon, "Propagation of single-mode and multi-mode terahertz radiation through a parallel-plate waveguide," J. Korean Phys. Soc. **53**, 1891-1896 (2008).